NJC

ROYAL SOCIETY OF CHEMISTRY

PAPER

View Article Online
View Journal | View Issue

Cite this: *New J. Chem.*, 2025, **49**, 19240

Enantiodifferentiation of chiral hydroxy acids *via* ^{19}F NMR†

Yilin Zeng,‡ Zixuan Ma‡ and Yanchuan Zhao *

Received 14th August 2025,
Accepted 21st October 2025

DOI: 10.1039/d5nj03288a

rsc.li/njc

We present a high-resolution ^{19}F NMR platform for the enantiodifferentiation of chiral hydroxy acids *via* a rapid three-component derivatization reaction between a ^{19}F-labeled chiral amine, 2-formylphenylboronic acid, and the hydroxy acid analyte. The probe design includes two different fluorinated groups ($-CF_3$ and $-OCF_3$), allowing for detection using dual-site ^{19}F readout. This dual-fluorine strategy markedly improves chiral resolution and minimizes signal overlap, a common limitation of conventional ^{1}H NMR approaches. The method simultaneously distinguishes up to ten chiral hydroxy acids within a single spectrum and allows accurate determination of enantiomeric excess, offering a versatile, efficient, and separation-free platform for the rapid chiral analysis of structurally diverse hydroxy acids.

Introduction

Chirality is a defining feature of many biologically relevant molecules, including amino acids, sugars, proteins, and nucleotides.[1] The two enantiomers of a chiral compound frequently display markedly different biological and pharmacological properties.[2] For example, dextropropoxyphene acts as an analgesic, whereas its mirror image, levopropoxyphene, functions as an antitussive agent.[3] In agrochemicals, *R*-(+)-chlorbufam exhibits nearly fourfold higher herbicidal activity than *S*-(−)-chlorbufam.[4] These examples highlight that the function and bioactivity of chiral compounds are intimately linked to their stereochemistry.[5] Chiral hydroxy acids, such as lactic, malic, and tartaric acids, occur widely in nature and play important roles in biological systems. In the food industry, the L/D lactic acid ratio serves as a key quality metric for fermented products.[6] In pharmaceuticals, the anticancer drug paclitaxel depends on the chirality of its key precursor, 2,3-dihydroxy-3-phenylpropionate, for therapeutic efficacy.[7] Given their critical roles, reliable and efficient methods for distinguishing hydroxy acid enantiomers are essential in food quality control, pharmaceutical production, and related fields.

The demand for accurate enantiomer differentiation spans chiral synthesis,[8] catalysis,[9,10] pharmacology, and biochemistry,[11] driving the development of diverse chiral recognition and separation techniques. Widely used methods include high-performance liquid chromatography (HPLC),[12–14] gas chromatography (GC),[15–17] capillary electrophoresis (CE),[18–20] and nuclear magnetic resonance (NMR) spectroscopy.[21–24] Among these, NMR offers several advantages: It enables rapid enantiopurity assessment and typically requires no physical separation of analytes.[25] As a result, NMR has been extensively applied to the analysis of chiral hydroxy acids, often by converting enantiomers into diastereomers through derivatization with chiral derivatizing agents (CDAs)[26–29] or complexation with chiral solvating agents (CSAs).[30–33] Quantitative enantiomer discrimination is then achieved by integrating distinct diastereomeric signals. Representative examples include Suryaprakash's three-component protocol employing 2-formylphenylboronic acid and [1,1-dinaphthyl]-2,2-diamine for ^{1}H NMR analysis of chiral acids,[34] Zhang's *R*-amino acid-derived carboxylic acid receptors for hydroxy acid analysis,[35] and Riguera's BINOL borate approach for absolute configuration determination.[36] More recently, Liu and coworkers utilized cinchona alkaloid dimers as CSAs to resolve aminobutylamine derivatives by ^{1}H NMR.[37] Despite these advances, ^{1}H NMR spectra often suffer from severe signal overlap between analytes and chiral auxiliaries, particularly when primary amines are used, hindering accurate determination of enantiomeric excess (ee).

To overcome the spectral crowding inherent to ^{1}H NMR–based chiral assays, a more selective detection modality is required. ^{19}F NMR offers several compelling advantages for chiral analysis: ^{19}F has 100% natural abundance, high receptivity, and a broad chemical shift dispersion, while being essentially absent from most biological matrices, resulting in negligible background signals. These attributes have enabled its successful application to the enantiodifferentiation of diverse functional classes, including amines, amino acids, alcohols, amides, sulfoxides, nitriles, and N-heterocycles,[38–43] as well as to the real-time monitoring of biological activity and metabolic processes.[44–46] Many reported ^{19}F NMR chiral

State Key Laboratory of Fluorine and Nitrogen Chemistry and Advanced Materials, Shanghai Institute of Organic Chemistry, University of Chinese Academy of Sciences, Chinese Academy of Sciences, 345 Ling-Ling Road, Shanghai 200032, China. E-mail: zhaoyanchuan@sioc.ac.cn

† Dedicated to Professor Resnati, celebrating a career in fluorine and noncovalent chemistry on the occasion of his 70th birthday.

‡ These authors contributed equally to this work.

sensing systems rely on a single fluorine source; however, the optimal chemical shift discrimination varies across analyte classes, and a fixed fluorine environment rarely delivers uniformly high resolution. We envision that integrating multiple spectroscopically distinct fluorine moieties into a single probe could provide multiple detection sites, thereby enhancing analyte scope and resolution. Herein, we report a ^{19}F NMR platform have two fluorine sources for the enantiodiscrimination of chiral hydroxy acids. The system is assembled *in situ* from a strategically designed optically pure ^{19}F-labeled chiral amine (**1**) bearing $-CF_3$ and $-OCF_3$ substituents, and *o*-formylphenylboronic acid (**2**). In the presence of a hydroxy acid, a rapid three-component condensation produces fluorinated diastereomeric boronate esters, driven by the strong affinity between phenylboronic acids and *cis*-vicinal hydroxyl groups (Scheme 1).[47] The distinct stereochemistry of each enantiomer alters the local magnetic environment of both fluorine sites, generating well-resolved ^{19}F NMR signals. Two fluorine labels with differential resolving ability enable high-confidence enantiodifferentiation across a broad range of hydroxy acids with exceptional resolution, enabling the simultaneous differentiation of multiple chiral hydroxy acids within complex mixtures.[48–50] In addition to being cost-effective, it circumvents the signal-overlap issues common in conventional ^{1}H NMR spectra, thereby allowing accurate determination of ee values for chiral acids using ^{19}F NMR.

Experimental

Preparation of NMR samples

Stock solutions of the analytes (15.4 mM in $CDCl_3$), compound **1** (7.7 mM in $CDCl_3$), and compound **2** (7.7 mM in $CDCl_3$) were prepared. For each measurement, 200 μL of the **1** solution (containing 1 mg of **1**), 100 μL of the analyte solution (containing 0.58–0.84 mg of analyte), and 200 μL of the **2** solution (containing 0.58 mg of **2**) were combined, mixed thoroughly to ensure rapid reaction, and immediately transferred to an NMR tube for ^{19}F{^{1}H} NMR analysis.

NMR measurements

^{19}F NMR spectra were acquired on a Bruker Avance NEO 600 spectrometer (565 MHz for ^{19}F) equipped with a BBFO probe at 298 K. Data were collected with a relaxation delay (D_1) of 1 s and 32 scans. For all ^{19}F NMR, proton decoupling was performed for simplifying the spectra, chemical shifts (δ) are reported in parts per million (ppm) All spectra were processed using MestReNova software. During this processing, we employed manual phase correction to ensure the accuracy of the spectral representation. Subsequently, integration of the peaks was performed manually to determine the ratio between peak areas.

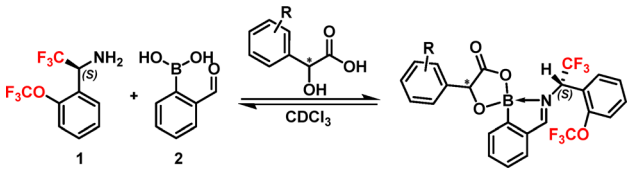

Scheme 1 ^{19}F NMR Chiral discrimination of hydroxy acids *via* a three-component reaction.

Results and discussion

We first examined the reaction between the $-CF_3$/$-OCF_3$-labeled chiral amine **1** and *o*-formylphenylboronic acid **2** (Fig. 1(a)). Previous studies have shown that **2** can efficiently couple with various amines, providing a versatile platform for chiral discrimination.[51,52] Upon mixing equimolar solutions of **1** and **2**, the ^{19}F NMR spectrum displayed a new set of signals (Fig. 1(d)), consistent with the formation of imine **3**. The condensation proceeded with high efficiency, converting nearly all of **1** to **3** under equimolar conditions (Fig. S1). The reaction was reversible: addition of excess 1-phenylethanamine to **3** regenerated free amine **1** (Fig. S2). To assess the chiral discrimination capability, we chose DL-3-phenyl-lactic acid ($\mathbf{A_1}$) as a model hydroxy acid

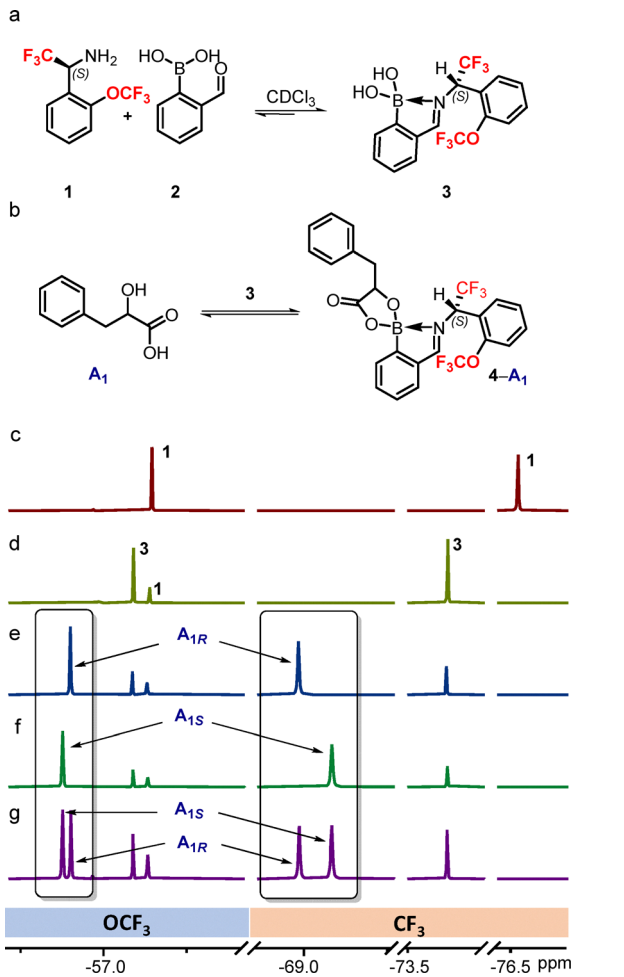

Fig. 1 (a) Reaction between **1** and **2** (7.7 mM each); (b) formation of boronic acid esters; (c) ^{19}F{^{1}H} NMR spectrum of ^{19}F-labeled amine **1**; (d) ^{19}F{^{1}H} NMR spectrum of **1** + **2**; (e) **1** + **2** + $\mathbf{A_{1R}}$; (f) **1** + **2** + $\mathbf{A_{1S}}$; (g) **1** + **2** + racemic $\mathbf{A_1}$. ^{19}F{^{1}H} NMR spectra were acquired on a Bruker Avance NEO 600 spectrometer (565 MHz for ^{19}F) equipped with a BBFO probe at 298 K. Data were collected with a relaxation delay (D_1) of 1 s and 32 scans.

(Fig. 1(b)). Treatment of **3** with either the (*R*)- or (*S*)- enantiomer of $\mathbf{A_1}$ yielded distinct ^{19}F NMR patterns (Fig. 1(e) and (f)), attributable to the formation of diastereomeric boronate esters. *In situ* ^{19}F NMR revealed only signals from **1**, **3**, and the desired boronic ester, while a transient, reversible broadening of the CF_3 signal upon mixing **1** with $\mathbf{A_1}$ vanished after addition of **2**, indicating that any weak acid–base interaction exerts minimal impact on the detection process (Fig. S9c). We also performed a titration experiment using $\mathbf{A_1}$ to confirm that the reaction is rapid and selective (Fig. S8). The minor residual signals of **1** and **3** in Fig. 1(d)–(g) reflect an equilibrium under limited analyte, as confirmed by titrations that diminish these signals with increasing $\mathbf{A_1}$ (Fig. S10). The chemical-shift differences between the enantiomeric adducts reflect the stereochemistry-dependent magnetic environment at each fluorine site. Analysis of a racemic mixture of $\mathbf{A_1}$ produced two signals that precisely matched those from the individual enantiomers (Fig. 1(g)), confirming the method's accuracy in distinguishing hydroxy acid enantiomers.

The specific equation for calculating the resolution (R_s).

$$R_s = \frac{\delta_A - \delta_B}{W_h(A) + W_h(B)} \quad (1)$$

To assess the generality of the method, we extended the study to hydroxy acids with diverse structural motifs (Fig. 2). To quantify enantiodiscrimination, we employed the resolution parameter (R_s, eqn (1)), where δ_A and δ_B are the ^{19}F chemical shifts of the enantiomeric pair, and W_h(A) and W_h(B) are the corresponding half-height line widths.[53] This metric is preferred

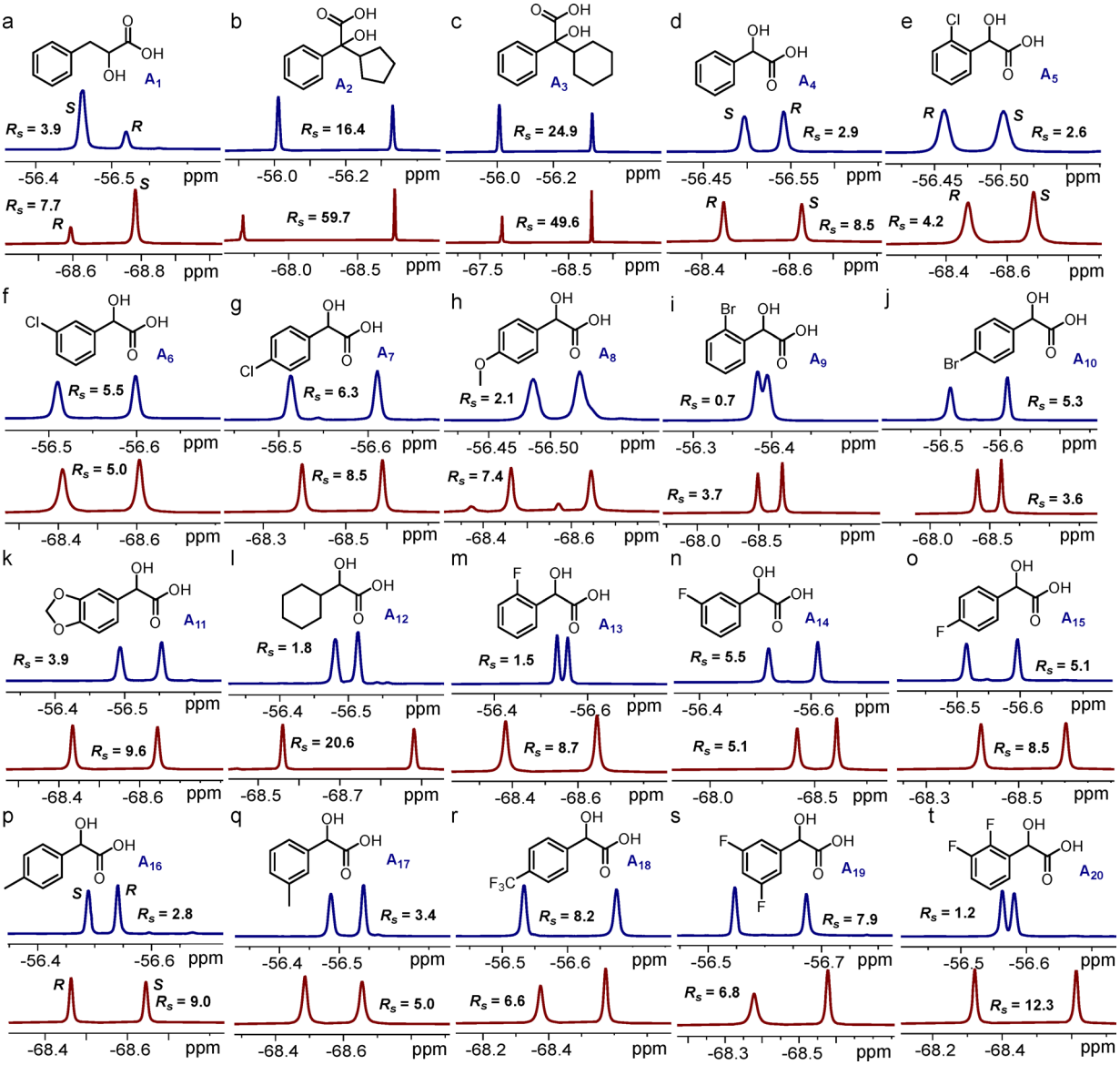

Fig. 2 (a)–(t) $^{19}F\{^1H\}$ NMR spectra of mixtures containing ^{19}F-labeled chiral amine **1** (7.7 mM), **2** (7.7 mM), and analytes (15.4 mM each) in $CDCl_3$. The signals for OCF_3 and CF_3 labels are shown in dark blue and dark red, respectively. $^{19}F\{^1H\}$ NMR spectra were acquired on a Bruker Avance NEO 600 spectrometer (565 MHz for ^{19}F) equipped with a BBFO probe at 298 K. Data were collected with a relaxation delay (D_1) of 1 s and 32 scans.

over simple $\Delta\delta$ values because ^{19}F line widths can vary substantially due to dynamic binding or conformational exchange, leading to peak broadening that compromises $\Delta\delta$ accuracy.[54] Using this definition, we evaluated a series of aromatic hydroxy acids ($\mathbf{A_1}$–$\mathbf{A_{20}}$) in both the –CF_3 (red traces) and –OCF_3 (blue traces) ranges at 298 K on a 600 MHz spectrometer (Fig. 2). In the CF_3 range, $\Delta\delta$ values were generally large enough to provide baseline separation, affording R_s values from 3.7 to 59.7. Bulky α-substituents, such as cyclopentyl ($\mathbf{A_2}$) and cyclohexyl ($\mathbf{A_3}$), gave the highest resolutions (R_s = 59.7 and 49.6, respectively), while phenyl substitution ($\mathbf{A_4}$) produced a modest R_s of 8.5. Comparison of $\mathbf{A_4}$ (phenyl) and $\mathbf{A_{12}}$ (cyclohexyl) suggests that increased steric bulk enhances chiral differentiation (R_s = 20.6 for $\mathbf{A_{12}}$), likely by restricting conformational flexibility in the boronate ester. *ortho*-Halogenation also influenced resolution: $\mathbf{A_9}$ (Br, R_s = 3.7) < $\mathbf{A_5}$ (Cl, R_s = 4.2) < $\mathbf{A_{13}}$ (F, R_s = 8.7), with the difluoro derivative $\mathbf{A_{20}}$ (R_s = 12.3) exceeding the unsubstituted $\mathbf{A_4}$. In contrast, the OCF_3 range displayed R_s values of 0.7–24.9. Here, bulky α-substituents produced mixed effects: $\mathbf{A_2}$ (R_s = 16.4) and $\mathbf{A_3}$ (R_s = 24.9) showed enhanced resolution relative to $\mathbf{A_4}$ (R_s = 2.9), whereas $\mathbf{A_{12}}$ (cyclohexyl) gave a reduced R_s of 1.8, possibly because the flexible cyclohexyl group lies further from the OCF_3 site, diminishing steric control. *ortho*-Halogenated derivatives generally exhibited lower resolution than $\mathbf{A_4}$, with no clear correlation to halogen electronegativity. We also performed additional experiments with hydroxy acids bearing long alkyl chains, which confirmed that our method enables their chiral discrimination (Fig. S6). Overall, the CF_3 label provided superior discriminatory power, delivering higher R_s values for most analytes. Nonetheless, the OCF_3 label still afforded clear chiral discrimination across the entire hydroxy acid set, underscoring the complementary nature of the dual-site design.

Leveraging the high resolution of our dual-site ^{19}F readout platform, we next examined its capacity for multiplexed enantiodiscrimination. A mixture of five structurally distinct hydroxy acids was prepared, including two enantiopure species ($\mathbf{A_1}$ and $\mathbf{A_{16}}$). Following addition of **1** and **2**, ^{19}F NMR spectra were acquired. In the CF_3 range, partial signal overlap was observed (Fig. S4). Strikingly, the OCF_3 label yielded ten well-resolved ^{19}F resonances, each unambiguously assigned to one enantiomer of a specific analyte (Fig. 3). This experiment demonstrates that the strategy enables simultaneous, unambiguous identification of multiple chiral hydroxy acids in a single measurement. Consistent with electronic/steric expectations, the bulky electron-withdrawing bromo substituent ($\mathbf{A_9}$) yields a weaker response than the electron-donating cyclohexyl group ($\mathbf{A_3}$), whereas fluorine substitution has little effect, likely due to its small size and efficient conjugation. Beyond enhancing throughput, the detection results of two fluorine sources provide complementary data streams, offering flexibility in detecting label selection for optimal resolution. Compared to conventional chiral HPLC, which requires sequential separations, our method affords rapid, separation-free discrimination of complex enantiomeric mixtures.

To evaluate the accuracy of ee determination, we selected 4-methylmandelic acid ($\mathbf{A_{16}}$) as a model analyte. Solutions with defined ee values were prepared and analyzed by ^{19}F NMR. Because $\mathbf{A_{16}}$ exhibits limited solubility in $CDCl_3$, 10 μL of triethylamine was added to each NMR tube to ensure complete dissolution. Control experiments varying the amount of triethylamine showed that lower amounts (*e.g.*, 5 μL) resulted in overlapping ^{19}F NMR signals, while higher amounts (15–20 μL) gave results comparable to those obtained with 10 μL (Fig. S7). Probe **1** contains two fluorinated sites (–CF_3 and –OCF_3), both capable of resolving the *R* and *S* enantiomers of $\mathbf{A_{16}}$; for quantification, the CF_3 range was selected due to its higher resolution. Enantiomeric excess values were obtained by integrating the relevant ^{19}F resonances and applying a correction factor to account for the slightly different complexation affinities of boronic acid **2** toward the two enantiomers. Across the ee range tested, the deviations between measured and actual values were less than 1.0% (Table 1 and Fig. S5). The mathematical foundation for

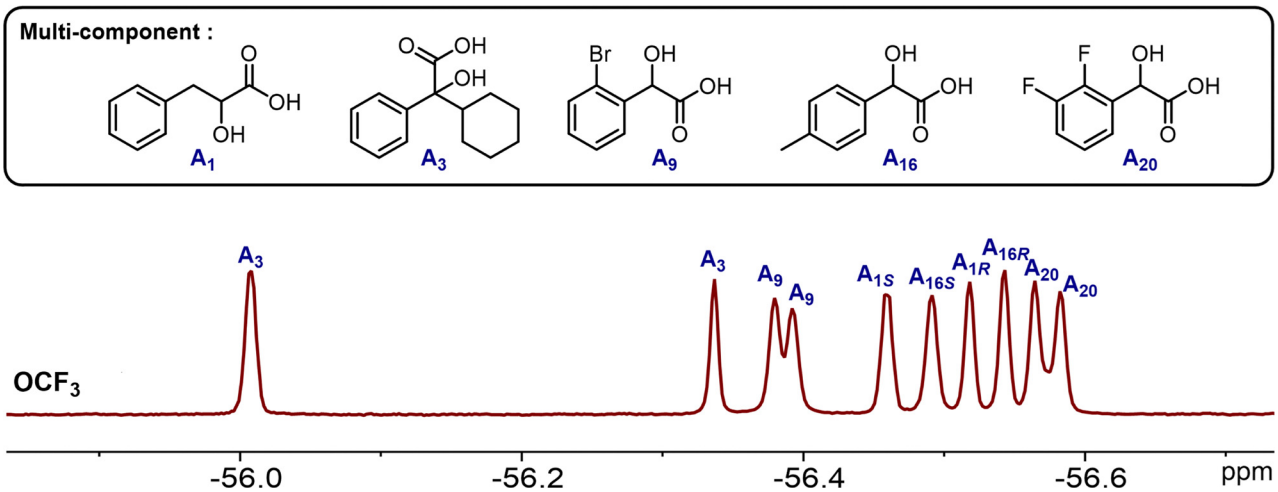

Fig. 3 $^{19}F\{^1H\}$ NMR spectra (OCF_3 range) of solutions containing chiral amine **1** (7.7 mM), **2** (7.7 mM), and analytes (15.4 mM each) in $CDCl_3$. $^{19}F\{^1H\}$ NMR spectra were acquired on a Bruker Avance NEO 600 spectrometer (565 MHz for ^{19}F) equipped with a BBFO probe at 298 K. Data were collected with a relaxation delay (D_1) of 1 s and 32 scans.

Table 1 Evaluation of the enantiomeric excess values using signals from CF_3 label

R-4-Methylmandelic acid ($\mathbf{A_{16}}$)		
Actual ee (%)	Calculated ee (%)	Deviation (%)
0	0	0
10.9	10.8	0.1
20.2	19.8	0.4
29.1	29.0	0.1
39.9	39.4	0.6
52.0	51.4	0.6
60.7	60.3	0.4
70.8	70.4	0.4
79.9	79.8	0.2
90.3	89.8	0.6

determining the ee value can be found in (Table S1). These results confirm that the method delivers precise and reliable ee determinations, underscoring its utility for rapid, quantitative chiral analysis of hydroxy acids.

Conclusions

In summary, we have developed a sensitive, precise, and separation-free ^{19}F NMR platform for the enantiodifferentiation of chiral hydroxy acids. The system is assembled *in situ* from *o*-formylphenylboronic acid and a chiral amine bearing $-CF_3$ and $-OCF_3$ labels, producing fluorinated boronate esters whose diastereomeric forms exhibit well-resolved, label-specific ^{19}F resonances. Dual-site ^{19}F readout overcomes the spectral overlap that often limits ^{1}H NMR methods, enabling the simultaneous discrimination of up to ten hydroxy acid enantiomers of diverse structures and the accurate quantification of enantiomeric excess. With its simplicity, broad analyte scope, and high throughput, this strategy provides a versatile tool for chiral analysis in pharmaceuticals, food chemistry, and bioanalytical applications, and its modular design should be readily adaptable to other classes of chiral molecules.

Author contributions

Yilin Zeng: investigation and writing – original draft; Zixuan Ma: investigation and writing – original draft; Yanchuan Zhao: review & editing.

Conflicts of interest

There are no conflicts to declare.

Data availability

The data supporting this article have been included as part of the SI. See DOI: https://doi.org/10.1039/d5nj03288a.

Acknowledgements

This work was supported by the Strategic Priority Research Program of the Chinese Academy of Sciences (XDB0590000), National Natural Science Foundation of China (22271305), and International Partnership Program of Chinese Academy of Sciences for future network (033GJHZ2022055FN). Y. Z. thanks Byungjin Koo for helpful discussion.

Notes and references

1 T. J. Ward and K. D. Ward, Chiral Separations: A Review of Current Topics and Trends, *Anal. Chem.*, 2012, **84**, 626–635.
2 A. Eaglesham, A. Scott and B. Petrie, Multi-Residue Enantioselective Analysis of Chiral Drugs in Freshwater Sediments, *Environ. Chem. Lett.*, 2020, **18**, 2119–2126.
3 I. W. Wainer, Three-Dimensional View of Pharmacology, *Am. J. Health-Syst. Pharm.*, 1992, **49**, S4–S8.
4 X. Yu, Z. Chen, L. Lv, M. Li and Q. Li, Evaluation of Chiral Pesticide Chlorbufam at the Enantiomeric Level: Absolute Configuration, Separation, Herbicidal Activity, and Degradation in Soil, *J. Agric. Food Chem.*, 2025, **73**, 5748–5756.
5 B. Kasprzyk-Hordern, Pharmacologically Active Compounds in the Environment and their Chirality, *Chem. Soc. Rev.*, 2010, **39**, 4466–4503.
6 A. Caligiani, M. Cirlini, G. Palla, R. Ravaglia and M. Arlorio, GC–MS Detection of Chiral Markers in Cocoa Beans of Different Quality and Geographic Origin, *Chirality*, 2007, **19**, 329–334.
7 M. C. Wani, H. L. Taylor, M. E. Wall, P. Coggon and A. T. McPhail, Plant Antitumor Agents. VI. Isolation and Structure of Taxol, a Novel Antileukemic and Antitumor Agent from Taxus Brevifolia, *J. Am. Chem. Soc.*, 1971, **93**, 2325–2327.
8 B. M. Trost, S. Malhotra, P. Koschker and P. Ellerbrock, Development of the Enantioselective Addition of Ethyl Diazoacetate to Aldehydes: Asymmetric Synthesis of 1,2-Diols, *J. Am. Chem. Soc.*, 2012, **134**, 2075–2084.
9 F. Gasparrini, M. Pierini, C. Villani, A. Filippi and M. Speranza, Induced-Fit in the Gas Phase: Conformational Effects on the Enantioselectivity of Chiral Tetra-Amide Macrocycles, *J. Am. Chem. Soc.*, 2008, **130**, 522–534.
10 T. N. Nguyen, P.-A. Chen, K. Setthakarn and J. A. May, Chiral Diol-Based Organocatalysts in Enantioselective Reactions, *Molecules*, 2018, **23**, 2317–2353.
11 Y. Chen, C. Chen and X. Wu, Dicarbonyl Reduction by Single Enzyme for the Preparation of Chiral Diols, *Chem. Soc. Rev.*, 2012, **41**, 1742–1753.
12 Y. Wang, J.-K. Chen, L.-X. Xiong, B.-J. Wang, S.-M. Xie, J.-H. Zhang and L.-M. Yuan, Preparation of Novel Chiral Stationary Phases Based on the Chiral Porous Organic Cage by Thiol-Ene Click Chemistry for Enantioseparation in HPLC, *Anal. Chem.*, 2022, **94**, 4961–4969.
13 C. Yuan, W. Jia, Z. Yu, Y. Li, M. Zi, L.-M. Yuan and Y. Cui, Are Highly Stable Covalent Organic Frameworks the Key to Universal Chiral Stationary Phases for Liquid and Gas Chromatographic Separations?, *J. Am. Chem. Soc.*, 2022, **144**, 891–900.
14 F. Ai, L. Li, S.-C. Ng and T. T. Y. Tan, Sub-1-Micron Mesoporous Silica Particles Functionalized with Cyclodextrin

Derivative for Rapid Enantioseparations on Ultra-High Pressure Liquid Chromatography, *J. Chromatogr. A*, 2010, **1217**, 7502–7506.

15 Y. Zhang and D. W. Armstrong, 4,6-Di-O-Pentyl-3-O-Trifluoroacetyl/Propionyl Cyclofructan Stationary Phases for Gas Chromatographic Enantiomeric Separations, *Analyst*, 2011, **136**, 2931–2940.

16 Y. Zhang, Z. S. Breitbach, C. Wang and D. W. Armstrong, The Use of Cyclofructans as Novel Chiral Selectors for Gas Chromatography, *Analyst*, 2010, **135**, 1076–1083.

17 B. Huang, K. Li, Q.-Y. Ma, T.-X. Xiang, R.-X. Liang, Y.-N. Gong, B.-J. Wang, J.-H. Zhang, S.-M. Xie and L.-M. Yuan, Homochiral Metallacycle Used as a Stationary Phase for Capillary Gas Chromatographic Separation of Chiral and Achiral Compounds, *Anal. Chem.*, 2023, **95**, 13289–13296.

18 Q. Fu, K. Zhang, D. Gao, L. Wang, F. Yang, Y. Liu and Z. Xia, *Escherichia Coli* Adhesive Coating as a Chiral Stationary Phase for Open Tubular Capillary Electrochromatography Enantioseparation, *Anal. Chim. Acta*, 2017, **969**, 63–71.

19 D. W. Armstrong, Y. Tang, T. Ward and M. Nichols, Derivatized Cyclodextrins Immobilized on Fused-Silica Capillaries for Enantiomeric Separations *via* Capillary Electrophoresis, Gas Chromatography, or Supercritical Fluid Chromatography, *Anal. Chem.*, 1993, **65**, 1114–1117.

20 R. Pérez-Míguez, M. L. Marina and M. Castro-Puyana, Capillary Electrophoresis Determination of Non-Protein Amino Acids as Quality Markers in Foods, *J. Chromatogr. A*, 2016, **1428**, 97–114.

21 W. Wang, X. Xia, G. Bian and L. Song, A Chiral Sensor for Recognition of Varied Amines Based on ^{19}F NMR Signals of Newly Designed Rhodium Complexes, *Chem. Commun.*, 2019, **55**, 6098–6101.

22 Y.-T. Chen, B. Li, J.-L. Chen and X.-C. Su, Simultaneous Discrimination and Quantification of Enantiomeric Amino Acids under Physiological Conditions by Chiral ^{19}F NMR Tag, *Anal. Chem.*, 2022, **94**, 7853–7860.

23 B. Huang, L. Xu, N. Wang, J. Ying, Y. Zhao and S. Huang, *Trans*-4-Fluoro-L-Proline: A Sensitive ^{19}F NMR Probe for the Rapid Simultaneous Enantiomeric Analysis of Multicomponent Amines, *Anal. Chem.*, 2022, **94**, 1867–1873.

24 Y.-T. Chen, B. Li, J.-L. Chen and X.-C. Su, Stereospecific Recognition of a Chiral Centre over Multiple Flexible Covalent Bonds by ^{19}F NMR, *Analyst*, 2023, **14**, 233–238.

25 V. Kumar Vashistha, Chiral Analysis of Pharmaceuticals Using NMR Spectroscopy: A Review, *Asian J. Org. Chem.*, 2022, **11**, e202200544.

26 J. A. Dale and H. S. Mosher, Nuclear Magnetic Resonance Enantiomer Reagents. Configurational Correlations *via* Nuclear Magnetic Resonance Chemical Shifts of Diastereomeric Mandelate, O-methylmandelate, and α-methoxy-α-trifluoromethylphenylacetate (MTPA) Esters, *J. Am. Chem. Soc.*, 1973, **95**, 512–519.

27 T. Yabuuchi and T. Kusumi, Phenylglycine Methyl Ester, a Useful Tool for Absolute Configuration Determination of Various Chiral Carboxylic Acids, *J. Org. Chem.*, 2000, **65**, 397–404.

28 A. M. Kelly, Y. Pérez-Fuertes, J. S. Fossey, S. L. Yeste, S. D. Bull and T. D. James, Simple Protocols for NMR Analysis of the Enantiomeric Purity of Chiral Diols, *Nat. Protoc.*, 2008, **3**, 215–219.

29 K. Bravo-Altamirano, L. Coudray, E. L. Deal and J.-L. Montchamp, Strategies for the Asymmetric Synthesis of H-Phosphinate Esters, *Org. Biomol. Chem.*, 2010, **8**, 5541.

30 N. H. Pham and T. J. Wenzel, A Water-Soluble Calix[4]-Resorcinarene with α-Methyl-l-Prolinylmethyl Groups as a Chiral NMR Solvating Agent, *J. Org. Chem.*, 2011, **76**, 986–989.

31 T. Kawanami, K. Ishizuka, H. Furuno, Y. Shiota, K. Yoshizawa and J. Inanaga, Efficient 1H NMR Chiral Discrimination of Sulfoxides Caused by the Dynamic Nature of (R,R)-3′,3″-biBINOL, *Tetrahedron: Asymmetry*, 2017, **28**, 1587–1590.

32 A. Recchimurzo, C. Micheletti, G. Uccello-Barretta and F. Balzano, A Dimeric Thiourea CSA for the Enantiodiscrimination of Amino Acid Derivatives by NMR Spectroscopy, *J. Org. Chem.*, 2021, **86**, 7381–7389.

33 A. Gualandi, S. Grilli, D. Savoia, M. Kwit and J. Gawroński, C-Hexaphenyl-Substituted Trianglamine as a Chiral Solvating Agent for Carboxylic Acids, *Org. Biomol. Chem.*, 2011, **9**, 4234–4241.

34 S. R. Chaudhari and N. Suryaprakash, Three-Component Chiral Derivatizing Protocols for NMR Spectroscopic Enantiodiscrimination of Hydroxy Acids and Primary Amines, *J. Org. Chem.*, 2012, **77**, 648–651.

35 D. Yang, X. Li, Y.-F. Fan and D.-W. Zhang, Enantioselective Recognition of Carboxylates: A Receptor Derived from α-Aminoxy Acids Functions as a Chiral Shift Reagent for Carboxylic Acids, *J. Am. Chem. Soc.*, 2005, **127**, 7996–7997.

36 F. Freire, E. Quiñoá and R. Riguera, In Tube Determination of the Absolute Configuration of α- and β-Hydroxy Acids by NMR *via* Chiral BINOL Borates, *Chem. Commun.*, 2008, 4147–4149.

37 M.-Y. Mo, X.-J. Wang, R.-Z. Shen, C.-Y. Hu, X.-C. Li, G.-W. Li and L.-T. Liu, Enantiospecific Analysis of Carboxylic Acids Using Cinchona Alkaloid Dimers as Chiral Solvating Agents, *Anal. Chem.*, 2024, **96**, 7487–7496.

38 C. Dong, Z. Xu, L. Wen, S. He, J. Wu, Q.-H. Deng and Y. Zhao, Tailoring Sensors and Solvents for Optimal Analysis of Complex Mixtures *Via* Discriminative ^{19}F NMR Chemosensing, *Anal. Chem.*, 2021, **93**, 2968–2973.

39 G. Gu, Z. Xu, L. Wen, J. Liang, C. Wang, X. Wan and Y. Zhao, Chirality Sensing of N-Heterocycles *via* ^{19}F NMR, *JACS Au*, 2023, **3**, 1348–1357.

40 Y. Li, L. Wen, H. Meng, J. Lv, G. Luo and Y. Zhao, Separation-Free Enantiodifferentiation with Chromatogram-like Output, *Cell Rep. Phys. Sci.*, 2020, **1**, 100100.

41 Y. Zeng, W. Bao, G. Gu and Y. Zhao, Enantiodifferentiation of Chiral Diols and Diphenols *via* Recognition-Enabled Chromatographic ^{19}F NMR, *Magn. Reson. Lett.*, 2024, 200112.

42 G. Gu, Y. Sun, C. Wang, Y. Zeng, T. Peng, B. Koo and Y. Zhao, Exploring the Chiral Match–Mismatch Effect in the Chiral Discrimination of Nitriles, *Anal. Chem.*, 2025, **97**, 1909–1916.

43 Z. Xu, C. Liu, S. Zhao, S. Chen and Y. Zhao, Molecular Sensors for NMR-Based Detection, *Chem. Rev.*, 2019, **119**, 195–230.

44 C.-Y. Cui, B. Li and X.-C. Su, Real-Time Monitoring of the Level and Activity of Intracellular Glutathione in Live Cells at Atomic Resolution by ^{19}F NMR, *ACS Cent. Sci.*, 2023, **9**, 1623–1632.

45 Z. Xu, C. Wang, S. He, J. Wu and Y. Zhao, Enhancing Molecular-Level Biological Monitoring with a Smart Self-Assembling ^{19}F-Labeled Probe, *Angew. Chem., Int. Ed.*, 2025, **64**, e202417112.

46 S. C. Song, C. Y. Wang, W. J. Bao, Z. C. Xu, J. Wu, L. Lin and Y. C. Zhao, High-Throughput ^{19}F NMR Chiral Analysis for Screening and Directed Evolution of Imine Reductases, *ACS Cent. Sci.*, 2025, **11**, 1094–1102.

47 X. Wu, Z. Li, X.-X. Chen, J. S. Fossey, T. D. James and Y.-B. Jiang, Selective Sensing of Saccharides Using Simple Boronic Acids and Their Aggregates, *Chem. Soc. Rev.*, 2013, **42**, 8032–8048.

48 Y. Zhao, G. Markopoulos and T. M. Swager, ^{19}F NMR Fingerprints: Identification of Neutral Organic Compounds in a Molecular Container, *J. Am. Chem. Soc.*, 2014, **136**, 10683–10690.

49 X. Wu, X. Tong, B. Huang and S. Huang, Novel Pseudo-Two-Dimensional ^{19}F NMR Spectroscopy for Rapid Simultaneous Detection of Amines in Complex Mixture, *Anal. Chem.*, 2024, **96**, 16818–16824.

50 N. Hamaguchi, R. Nishizawa, M. Ikeda, M. Yokoyama, H. Suzuki, K. Matsumoto, T. Ohta and Y. Oe, Primary Amine Discrimination Using a ^{19}F NMR Reporter Bearing Two Different Fluorine-Containing Moieties, *ChemistrySelect*, 2024, **9**, e202303190.

51 R. R. Groleau, R. S. L. Chapman, H. Ley-Smith, L. Liu, T. D. James and S. D. Bull, A Three-Component Derivatization Protocol for Determining the Enantiopurity of Sulfinamides by ^{1}H and ^{19}F NMR Spectroscopy, *J. Org. Chem.*, 2020, **85**(2), 1208–1215.

52 R. R. Groleau, R. S. L. Chapman, J. P. Lowe, C. L. Lyall, G. Kociok-Köhn, T. D. James and S. D. Bull, BINOL as a Chiral Solvating Agent for Sulfiniminoboronic Acids, *Anal. Chem.*, 2023, **95**, 16801–16809.

53 H. H. Li, Z. C. Xu, S. Q. Zhang, Y. S. Jia and Y. C. Zhao, Construction of Lewis Pairs for Optimal Enantioresolution *via* Recognition-Enabled ''Chromatographic'' ^{19}F NMR Spectroscopy, *Anal. Chem.*, 2022, **94**, 2023–2031.

54 J. Weng, L. Wen, G. Gu, W. Bao, J. Wu and Y. Zhao, Tailoring the Performance of ^{19}F-Labeled Probes *via* Dynamic Covalent Chemistry for Improved Chiral Discrimination, *Anal. Chem.*, 2024, **96**, 13551–13556.

